

CHEMICALLY REACTING JEFFREY FLUID FLOW OVER A DEFORMABLE POROUS LAYER WITH ENTROPY GENERATION ANALYSIS

Utpal Jyoti DAS

Department of Mathematics, Gauhati University, Guwahati-781014, INDIA

E-mail: utpaljyotidas@yahoo.co.in

Entropy generation of a steady Jeffrey fluid flow over a deformable vertical porous layer is analysed with consideration of a first-order chemical reaction and thermal diffusion. The porous material is modelled as a homogeneous binary mixture of fluid and solid phases where each point in the binary mixture is occupied concurrently by the fluid and solid. The combined phenomenon of solid deformation and fluid movement is taken into account. The impact of relevant parameters on the fluid velocity, solid displacement, temperature and concentration profiles is discussed. It is noticed that the Jeffrey fluid parameter enhances the entropy generation number, fluid velocity and solid displacement profiles, but a reverse effect is seen for the Bejan number. Further, entropy generation, fluid velocity and solid displacement reduce due to the higher estimates of the chemical reaction parameter, while the Bejan number enhances.

Key words: deformable porous layer, Jeffrey fluid, entropy generation, Bejan number, thermal diffusion.

1. Introduction

The flow of fluids in the porous media with or without chemical reaction has attracted the attention of researchers due to the extensive range of applications in the engineering and technological processes [1]. In recent times, Dutta and Kalita [2] studied double-diffusive characteristics of natural convection through a porous annulus. Alhadhrami *et al.* [3] studied the chemically reactive fluid flow of a non-Newtonian fluid through a porous medium with non-equilibrium surface conditions. Kalita and Choudhury [4] presented the chemically reacting thermophoretic viscous MHD flow in a converging channel through a porous medium. Several authors [5-9] have presented similar research. In the above studies, the porous layer was taken as fixed. But, the study of flow in a deformable porous layer is also important because of broad applications in the fields of biology [10], geology and tissue mechanics for articular cartilage. Biot [11] developed the theory of deformation and acoustic propagation of fluid. An important investigation on fluid flow phenomena over a thin deformable porous material was carried out by Barry *et al.* [12]. Again, Sreenadh *et al.* [13] investigated the free convective flow of a Jeffrey fluid through a vertical deformable porous stratum. Murthy [14] presented the impact of heat and mass transfer on an MHD flow of a Casson liquid in a deformable porous medium considering slip effects.

Entropy generation analysis of a system gives an important insight into the power consumption due to thermodynamic losses. Optimization of power for a system of fluid motion is achieved by minimizing the entropy generation. Bejan [15] explained the thermodynamic properties and procedure for optimization of entropy generation for a fluid flow system. Egunjobi and Makinde [16] analyzed the entropy generation for an MHD flow of a Newtonian fluid in a channel. Das and Jana [17] presented the entropy generation due to an MHD flow through a porous channel with Navier slip. Shit *et al.* [18] made the entropy generation analysis on an MHD flow in an exponentially stretching sheet. Sreenadh *et al.* [19] presented the entropy generation analysis for an MHD Newtonian fluid flow through a vertical porous layer. Several authors, Hayat *et al.* [20], Abdelhameed [21], Panigrahi *et al.* [22], Ullah *et al.* [23] analysed the entropy generation in different fluid flow systems.

The objective of this paper is to study the entropy generation of Jeffrey fluid flow through a deformable porous channel considering a first-order chemical reaction and Soret effect. The expression representing solutions for fluid velocity, solid displacement, temperature and concentration profiles are obtained analytically. This study extends the work of Sreenadh *et al.* [13] by adding entropy generation, chemical reaction effect and thermal diffusion effect.

2. Mathematical formulation

Consider a steady fully developed flow of an incompressible Jeffrey fluid through a deformable, vertical porous layer in the presence of a first-order chemical reaction and thermal diffusion. The porous material is taken as a continuous, homogeneous and isotropic mixture of fluid and solid phases where each point in the binary mixture is occupied concurrently by the fluid and solid (Barry *et al.* [12]). The \bar{x} - axis is taken along the midway of the stratum and the \bar{y} -axis at right angles to it (Fig1.). The walls of the channel are at a distance $2h$. The heat is generated inside the fluid by viscous and Darcy dissipations.

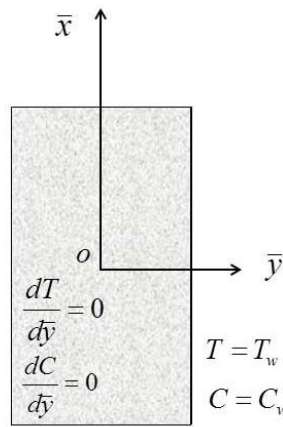


Fig.1. Physical model.

The governing equations of the flow, following Barry *et al.* [12] and Sreenadh *et al.* [13] become

$$\frac{2\mu_a}{I + \lambda_1} \frac{\partial^2 \bar{v}}{\partial \bar{y}^2} - K\bar{v} + g\rho^f \beta(T - T_0) + g\rho^f \beta_C(C - C_0) - \phi_f \frac{\partial \bar{P}}{\partial \bar{x}} = 0, \quad (2.1)$$

$$\mu \frac{\partial^2 \bar{u}}{\partial \bar{y}^2} + K\bar{v} - (I - \phi_f) \frac{\partial \bar{P}}{\partial \bar{x}} = 0, \quad (2.2)$$

$$\frac{\partial^2 \bar{T}}{\partial \bar{y}^2} + \frac{K}{K_0} \bar{v}^2 + \frac{2\mu_a}{(I + \lambda_1)K_0} \left(\frac{\partial \bar{v}}{\partial \bar{y}} \right)^2 = 0, \quad (2.3)$$

$$D \frac{\partial^2 C}{\partial \bar{y}^2} - \bar{R}(C - C_0) + D_T \frac{\partial^2 T}{\partial \bar{y}^2} = 0. \quad (2.4)$$

The boundary conditions are (Sreenadh *et al.* [13])

$$\begin{aligned} \bar{v} = 0, \quad \bar{u} = 0, \quad T = T_w, \quad C = C_w \quad \text{at} \quad \bar{y} = h, \\ \frac{d\bar{v}}{d\bar{y}} = 0, \quad \frac{d\bar{u}}{d\bar{y}} = 0, \quad \frac{dT}{d\bar{y}} = 0, \quad \frac{dC}{d\bar{y}} = 0 \quad \text{at} \quad \bar{y} = 0 \end{aligned} \quad (2.5)$$

where \bar{u} is the solid displacement, \bar{v} is the fluid velocity and λ_1 is the Jeffrey fluid parameter. The other variables are explained in Nomenclature.

The following non-dimensional quantities are introduced:

$$\begin{aligned} y = \frac{\bar{y}}{h}, \quad v = \frac{\bar{v}}{U}, \quad u = \frac{\bar{u}\mu}{2\mu_a U}, \quad x = \frac{\bar{x}}{h}, \quad \theta = \frac{T - T_0}{T_w - T_0}, \quad \phi = \frac{C - C_0}{C_w - C_0}, \\ P = \frac{h\bar{P}}{2\mu_a U}, \quad \mu_f = 2\mu_a, \quad \delta = \frac{Kh^2}{2\mu_a}, \quad Gr = \frac{g\beta\rho^f h^2 (T_w - T_0)}{2\mu_a U}, \\ Gc = \frac{g\beta_C \rho^f h^2 (C_w - C_0)}{2\mu_a U}, \quad Br = \frac{2\mu_a U^2}{K_0(T_w - T_0)}, \quad R = \frac{\bar{R}h^2}{D}, \quad Sc = \frac{\nu_f}{D}, \\ Sr = \frac{D_T(T_w - T_0)}{\nu_f(C_w - C_0)}. \end{aligned} \quad (2.6)$$

Using (2.6), Eqs (2.1)-(2.4), become

$$\frac{1}{(1 + \lambda_1)} \frac{d^2 v}{dy^2} - \delta v + Gr\theta + Gr_c\phi - \phi_f P = 0, \quad (2.7)$$

$$\frac{d^2 u}{dy^2} + \delta v - (1 - \phi_f)P = 0, \quad (2.8)$$

$$\frac{d^2 \theta}{dy^2} + \frac{Br}{(1 + \lambda_1)} \left(\frac{dv}{dy} \right)^2 + Br\delta v^2 = 0, \quad (2.9)$$

$$\frac{d^2 \phi}{dy^2} - R\phi + SrSc \frac{d^2 \theta}{dy^2} = 0, \quad (2.10)$$

with restrictions

$$\begin{aligned} v = 0, \quad u = 0, \quad \theta = 1, \quad \phi = 1 \quad \text{at} \quad y = 1, \\ \frac{dv}{dy} = 0, \quad \frac{du}{dy} = 0, \quad \frac{d\theta}{dy} = 0, \quad \frac{d\phi}{dy} = 0 \quad \text{at} \quad y = 0 \end{aligned} \quad (2.11)$$

where Br, R, Sc, Sr, Gr and Gc are the Brinkman number, chemical reaction parameter, Schmidt number, Soret number, thermal Grashof number and solutal Grashof number, respectively.

Equations (2.7)-(2.10), cannot be solved in closed form. So, to solve them, for $Br \ll 1$, neglecting the superior powers Br , we may take

$$(v, u, \theta, \varphi) = ((v_0, u_0, \theta_0, \varphi_0) + Br((v_1, u_1, \theta_1, \varphi_1))). \quad (2.12)$$

Using Eq.(2.12) in Eqs (2.7)-(2.10) and equating to zeroth-order and first-order of Br , we obtain

$$\frac{1}{(1+\lambda_1)} \frac{d^2 v_0}{dy^2} - \delta v_0 + Gr \theta_0 + Gr c \varphi_0 - \varphi_f P = 0, \quad (2.13)$$

$$\frac{d^2 u_0}{dy^2} + \delta v_0 - (1 - \varphi_f) P = 0, \quad (2.14)$$

$$\frac{d^2 \theta_0}{dy^2} = 0, \quad (2.15)$$

$$\frac{d^2 \varphi_0}{dy^2} - R \varphi_0 + SrSc \frac{d^2 \theta_0}{dy^2} = 0, \quad (2.16)$$

$$\frac{1}{(1+\lambda_1)} \frac{d^2 v_1}{dy^2} - \delta v_1 + Gr \theta_1 + Gr c \varphi_1 = 0, \quad (2.17)$$

$$\frac{d^2 u_1}{dy^2} + \delta v_1 = 0, \quad (2.18)$$

$$\frac{d^2 \theta_1}{dy^2} + \frac{1}{(1+\lambda_1)} \left(\frac{dv_0}{dy} \right)^2 + \delta v_0^2 = 0, \quad (2.19)$$

$$\frac{d^2 \varphi_1}{dy^2} - R \varphi_1 + SrSc \frac{d^2 \theta_1}{dy^2} = 0, \quad (2.20)$$

with conditions

$$\begin{aligned} v_0 = v_1 = 0, \quad u_0 = u_1 = 0, \quad \theta_0 = 1, \quad \theta_1 = 0, \quad \varphi_0 = 1, \quad \varphi_1 = 0 \quad \text{at } y = 1, \\ \frac{dv_0}{dy} = \frac{dv_1}{dy} = 0, \quad \frac{du_0}{dy} = \frac{du_1}{dy} = 0, \quad \frac{d\theta_0}{dy} = \frac{d\theta_1}{dy} = 0, \quad \frac{d\varphi_0}{dy} = \frac{d\varphi_1}{dy} = 0 \quad \text{at } y = 0. \end{aligned} \quad (2.21)$$

Solving the Eqs (2.13)-(2.20) under conditions (2.21), we get

$$v_0 = A_3 \left[\exp\{-y\sqrt{\delta(I+\lambda_1)}\} + \exp\{y\sqrt{\delta(I+\lambda_1)}\} \right] + A_4 \left[\exp\{-y\sqrt{R}\} + \exp\{y\sqrt{R}\} \right] + A_5, \quad (2.22)$$

$$v_1 = A_{81} \exp\{-2\delta(I+\lambda_1)y\} + A_{82} \exp\{2\delta(I+\lambda_1)y\} + A_{83} \exp\{-2y\sqrt{R}\} + A_{84} \exp(2y\sqrt{R}) + A_{85} \exp\{-(\delta+\sqrt{R})y\} + A_{86} \exp\{(-\delta+\sqrt{R})y\} + A_{87} \exp\{(\delta-\sqrt{R})y\} + A_{88} \exp\{(\delta+\sqrt{R})y\} + A_{89} \exp(-y\sqrt{R}) + A_{90} \exp(y\sqrt{R}) + A_{91} \exp(-y\delta) + A_{92} \exp(y\delta) + A_{93}y + A_{94}, \quad (2.23)$$

$$u_0 = A_{119}y^2 + A_{120} \exp(-y\delta) + A_{121} \exp(y\delta) + A_{122} \exp(-y\sqrt{R}) + A_{123} \exp(y\sqrt{R}) + A_{124}y + A_{125}, \quad (2.24)$$

$$u_1 = A_{140} \exp(-2y\delta) + A_{141} \exp(2y\delta) + A_{142} \exp(-2y\sqrt{R}) + A_{143} \exp(2y\sqrt{R}) + A_{144} \exp\{-(\delta+\sqrt{R})y\} + A_{145} \exp\{(-\delta+\sqrt{R})y\} + A_{146} \exp\{(\delta-\sqrt{R})y\} + A_{147} \exp\{(\delta+\sqrt{R})y\} + A_{148} \exp(-y\sqrt{R}) + A_{149} \exp(y\sqrt{R}) + A_{150}y^3 + A_{151}y^2 + A_{152}y + A_{153} \exp(y\delta) + A_{154}y + A_{155}, \quad (2.25)$$

$$\theta_0 = I, \quad (2.26)$$

$$\theta_1 = A_{38} \exp\{-2\delta(I+\lambda_1)y\} + A_{39} \exp\{2\delta(I+\lambda_1)y\} + A_{40} \exp(-2y\sqrt{R}) + A_{41} \exp(2y\sqrt{R}) + A_{42} \exp\left[\left\{\delta(I+\lambda_1)+\sqrt{R}\right\}y\right] + A_{43} \exp\left[\left\{-\delta(I+\lambda_1)+\sqrt{R}\right\}y\right] + A_{44} \exp\left[\left\{\delta(I+\lambda_1)-\sqrt{R}\right\}y\right] + A_{45} \exp\left[\left\{\delta(I+\lambda_1)+\sqrt{R}\right\}y\right] + A_{46} \exp\{-\delta(I+\lambda_1)y\} + A_{47} \exp\{\delta(I+\lambda_1)y\} + A_{48} \exp(-y\sqrt{R}) + A_{49} \exp(y\sqrt{R}) + A_{46} \exp\{-\delta(I+\lambda_1)y\} + A_{50}y + A_{51}, \quad (2.27)$$

$$\phi_0 = A_1 \left\{ \exp(-y\sqrt{R}) + \exp(y\sqrt{R}) \right\}, \quad (2.28)$$

$$\phi_1 = A_{52} \exp\{-2\delta(I+\lambda_1)y\} + A_{53} \exp\{2\delta(I+\lambda_1)y\} + A_{54} \exp(-2y\sqrt{R}) + A_{55} \exp(2y\sqrt{R}) + A_{56} \exp\left[\left\{\delta(I+\lambda_1)+\sqrt{R}\right\}y\right] + A_{57} \exp\left[\left\{-\delta(I+\lambda_1)+\sqrt{R}\right\}y\right] + A_{58} \exp\left[\left\{\delta(I+\lambda_1)-\sqrt{R}\right\}y\right] + A_{59} \exp\left[\left\{\delta(I+\lambda_1)+\sqrt{R}\right\}y\right] + A_{60} \exp\{-\delta(I+\lambda_1)y\} + A_{61} \exp\{\delta(I+\lambda_1)y\} + A_{62}y \exp(-y\sqrt{R}) + A_{63}y \exp(y\sqrt{R}) + A_{64}. \quad (2.29)$$

The constants A_i ($i = 1$ to 155) are not presented here for the sake of brevity.

3. Results and discussion

In this section, the impact of physical parameters on the fluid velocity, solid displacement, temperature, concentration, entropy generation number and Bejan number is discussed.

In the absence of a chemical reaction and $Sr = 0$, the present problem reduces to the problem of Sreenadh *et al.*[13] and the present results have been in good concurrence with the results of Sreenadh *et al.* [13].

For the calculation, the following values are assigned to the physical parameters:

$$\lambda_1 = 0.2, \quad \phi_f = 0.7, \quad \phi_s = 0.3, \quad \delta = 0.7, \quad Br = 0.02, \quad R = 1,$$

$$Gr = 0.5, \quad Gc = 0.5, \quad P = -5, \quad Sr = 1, \quad Sc = 1.$$

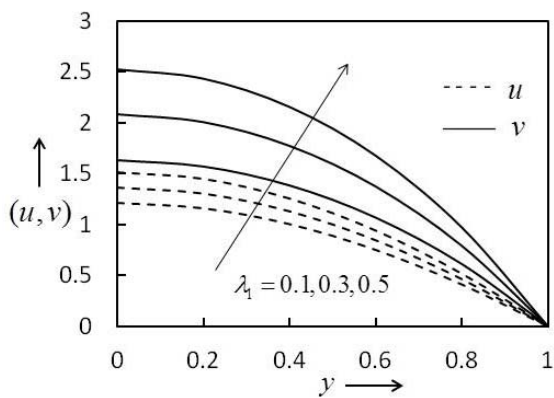


Fig.2. Effect of λ_1 on u and v .

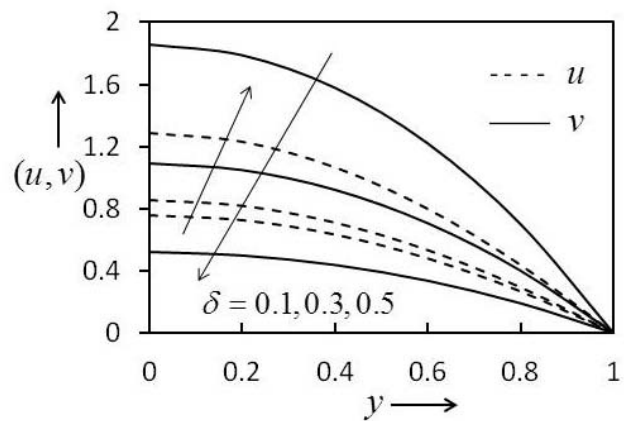


Fig.3. Effect of δ on u and v .

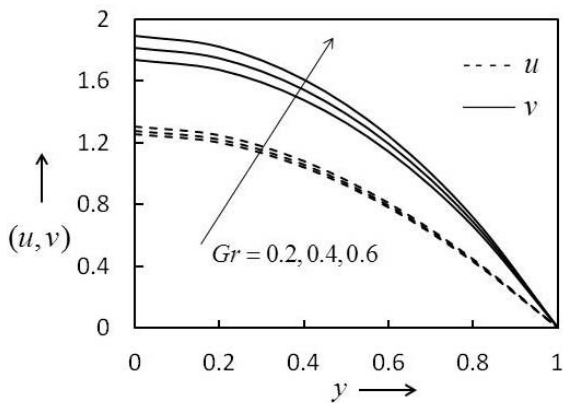


Fig.4. Effect of Gr on u and v .

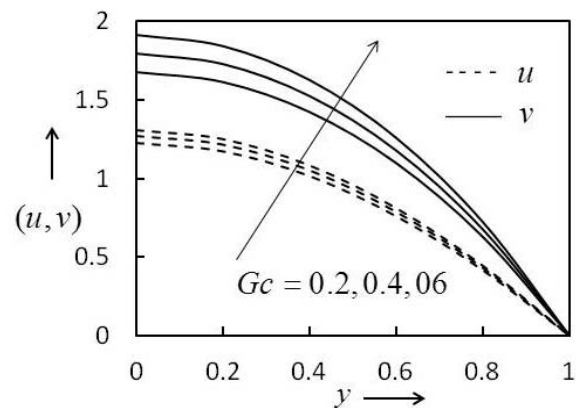


Fig.5. Effect of Gc on u and v .

Figures 2-9 represent the fluid velocity and solid displacement profiles for various values of the Jeffrey fluid parameter (λ_1), drag parameter (δ), thermal Grashof number (Gr), solutal Grashof number (Gc), chemical reaction parameter (R), pressure gradient parameter (P), volume fraction component of fluid phase (ϕ_f) and Soret number (Sr), respectively. Figure 2 shows that the effect of the increasing Jeffrey fluid parameter enhances both the fluid velocity and solid displacement profiles. Thus, the polymer flow significantly accelerates with an increase in the relaxation time (or decreasing retardation time). This

model reduces to a Newtonian model when $\lambda_j \rightarrow 0$. Figure 3 shows that the impact of the drag parameter increases solid displacement while the fluid velocity decreases. Physically, it can be explained that the drag force reduces the fluid velocity and there is less fluid momentum to impede the solid displacement. Thus, the fluid velocity reduces and solid displacement increases as the drag is smaller. From Figure 4 it is observed that increasing Gr leads to an enhancement of both the fluid velocity and solid displacement. The similar impact can be achieved by increasing Gc as shown in Fig.5.

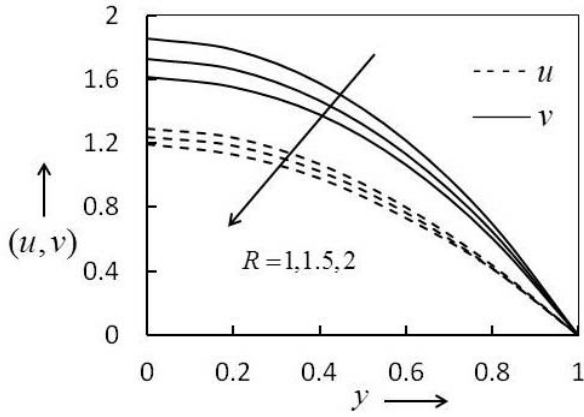


Fig.6. Effect of R on u and v .

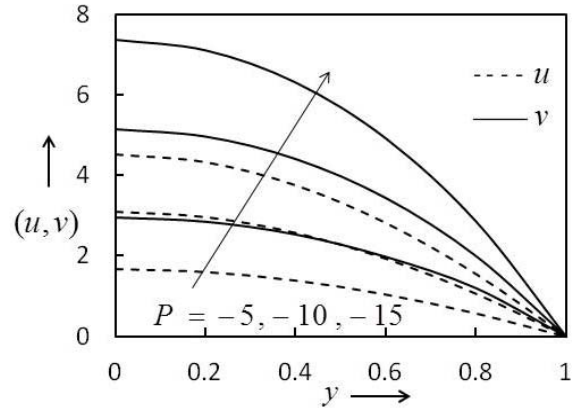


Fig.7. Effect of P on u and v .

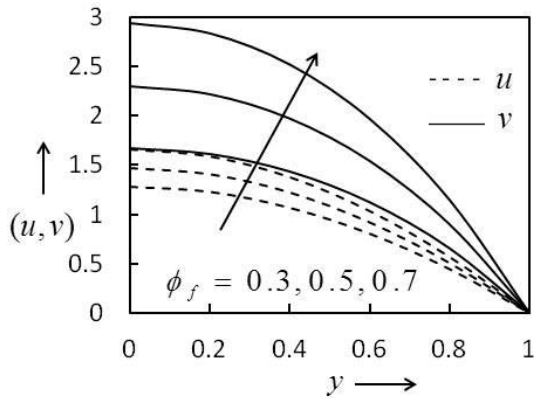


Fig.8. Effect of ϕ_f on u and v .

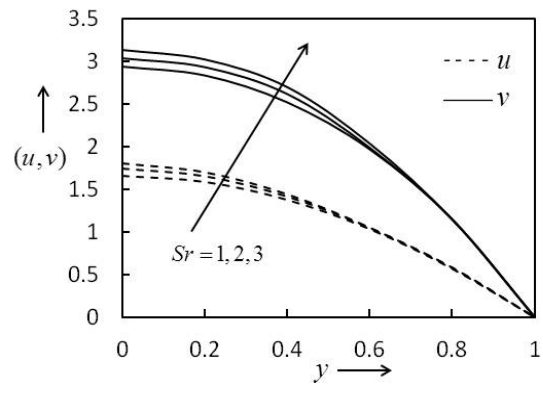


Fig.9. Effect of Sr on u and v .

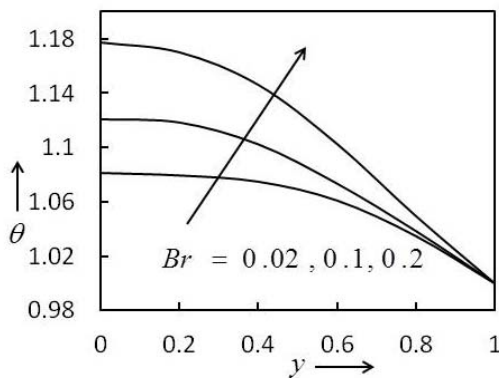


Fig.10. Effect of Br on temperature.

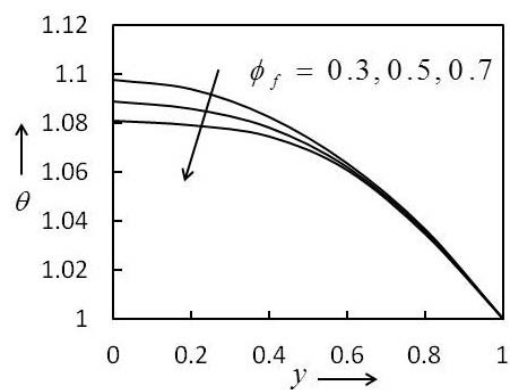


Fig.11. Effect of ϕ_f on temperature.

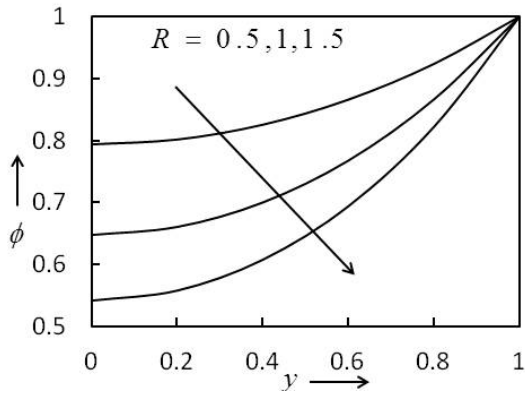


Fig.12. Effect of R on concentration.

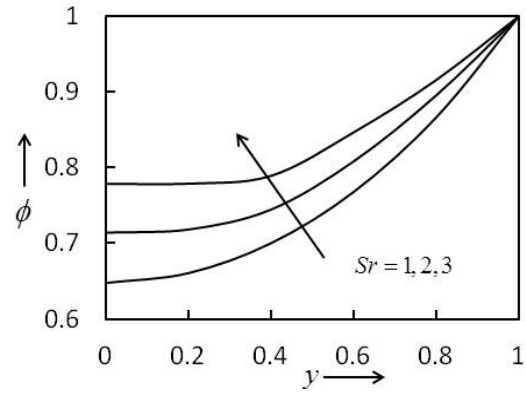


Fig.13. Effect of Sr on concentration.

Physically, it can be said that when the buoyancy force (thermal or concentration) is more dominant in comparison to hydrodynamic viscous force then it promotes both the solid displacement and fluid velocity. Figure 6 shows that the fluid velocity and solid displacement decelerate due to the higher estimates of the chemical reaction parameter. Figure 7 shows that the rising of the pressure gradient (P) reduces the fluid velocity and solid displacement. This can be physically explained considering that an increase in the pressure gradient makes the system thicker and consequently decreases the speed of the solid displacement and fluid velocity. Figure 8 shows that the fluid velocity and solid displacement is growing with an increasing volume fraction coefficient of the fluid. Figure 9 indicates that the fluid velocity and solid displacement rise as the Soret number (Sr) increases. Figure 10 reveals that the temperature profile enhances with the growing Brinkman number. This is because of the fact that the Brinkman number enhances the effect of viscous dissipation and thus tends to increase the temperature. Figure 11 shows that temperature reduces due to an increase in the volume fraction parameter of the fluid.

The effect of the chemical reaction parameter (R) and Soret number (Sr) on the concentration profile (ϕ) is shown in Figs 12 and 13. The concentration reduces for higher values of the chemical reaction parameter and as opposed to the Soret number.

3.1 Entropy generation

Following Das and Jana [20], entropy generation inside a deformable porous layer is

$$E_G = \frac{K_0}{T_0^2} \left(\frac{dT}{d\bar{y}} \right) + \frac{2\mu_a}{T_0(I + \lambda_I)} \left(\frac{d\bar{v}}{d\bar{y}} \right)^2 + \frac{K}{T_0} \bar{v}^2. \tag{3.1}$$

The dimensionless entropy generation number N_S is given as

$$N_S = \frac{T_0^2 a^2 E_G}{\kappa(T_w - T_0)^2} = \left(\frac{d\theta}{dy} \right)^2 + \frac{Br}{\Omega(I + \lambda_I)} \left[\left(\frac{dv}{dy} \right)^2 + \delta v^2 \right] = N_1 + N_2 \tag{3.2}$$

where $N_1 = \left(\frac{d\theta}{dy}\right)^2$ is entropy generation owing to heat transfer, $N_2 = \frac{Br}{\Omega} \left[\left(\frac{dv}{dy}\right)^2 + v^2 \right]$ is entropy generation owing to fluid friction and $\Omega = \frac{T_w - T_0}{T_0}$ is the dimensionless temperature difference. The Bejan number is $Be = \frac{N_1}{N_s} = \frac{I}{I + \Phi}$, where $\Phi = \frac{N_2}{N_1}$ is the irreversibility ratio.

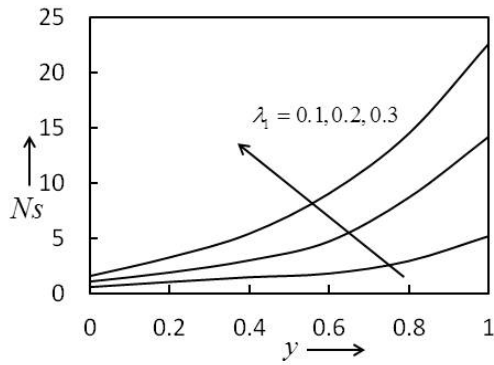


Fig.14. Effect of λ_1 on entropy generation.

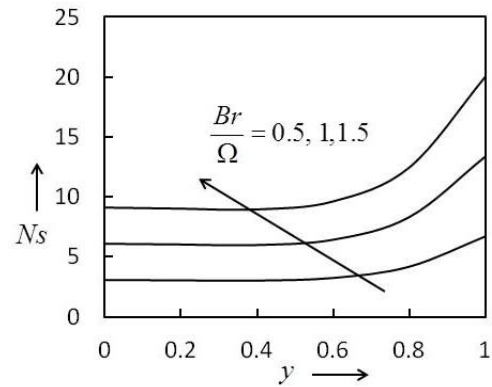


Fig.15. Effect of $\frac{Br}{\Omega}$ on entropy generation.

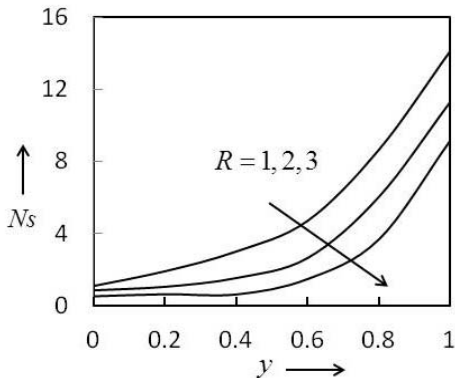


Fig.16. Effect of R on entropy generation.

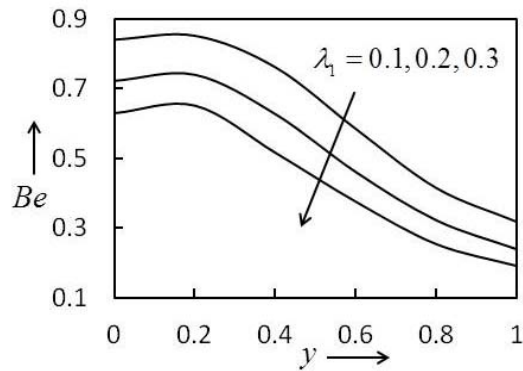


Fig.17. Effect of λ_1 on Bejan number.

The impact of the Jeffrey fluid parameter, $\frac{Br}{\Omega}$ and chemical reaction parameter on entropy generation is presented in Figs 14-16. It is observed that the entropy generation number (N_s) within the deformable porous layer increases when the Jeffrey fluid parameter or $\frac{Br}{\Omega}$ or chemical reaction parameter amplify. For irreversibility analysis the pair $\frac{Br}{\Omega}$ is a key parameter as it gives the relative significance of viscous effects and temperature gradient entropy generation. Thus, the enhancement in $\frac{Br}{\Omega}$ will lead to the

boost in the fluid friction irreversibility (N_2) as the entropy generation number enlarges when $\frac{Br}{\Omega}$ amplifies. Figures 17-19 represent the influence of λ_1 , $\frac{Br}{\Omega}$ and R , on the Bejan number (Be), respectively. It reveals that Be increases with an increase in λ_1 (Fig.17) or $\frac{Br}{\Omega}$ (Fig.18), while a reverse effect is seen for the chemical reaction parameter (Fig.19).

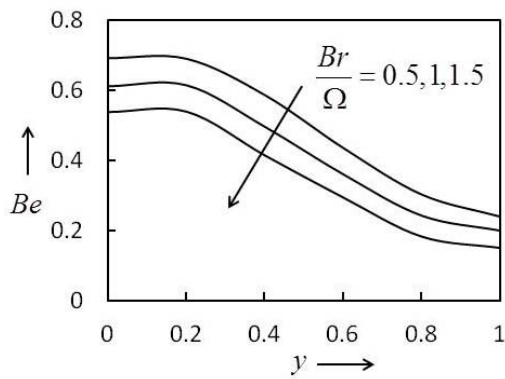


Fig.18. Effect of $\frac{Br}{\Omega}$ on Bejan number.

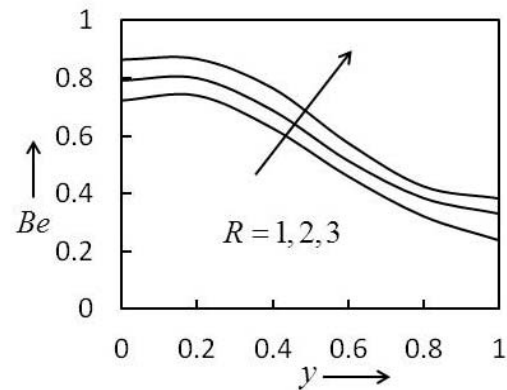


Fig.19. Effect of R on Bejan number.

4. Conclusions

Main observations of the above study are as follows:

- The Jeffrey fluid parameter enhances fluid velocity and the solid displacement significantly.
- An increase in the drag parameter causes a reduction in the fluid velocity, while the solid displacement of the two-phase medium rises.
- The motion of the fluid flow and solid displacement can be controlled by increasing the pressure gradient.
- To increase the solid displacement and fluid velocity of the two-phase medium, the Soret number or solutal Grashof number or thermal Grashof number or volume fraction parameter may be increased.
- An increase in the chemical reaction parameter causes a reduction in the fluid velocity and solid displacement.
- To increase the temperature of the system the Brinkman number may be increased or the volume fraction parameter may be decreased.
- To increase concentration profile of the system the chemical reaction parameter may be decreased or the Soret number may be increased.
- The entropy generation number may be increased by increasing the Jeffrey fluid parameter or the pair $\frac{Br}{\Omega}$, while it decreases with increasing the chemical reaction parameter.
- The Bejan number may be decreased by increasing the Jeffrey fluid parameter or the pair $\frac{Br}{\Omega}$, while it increases with increasing chemical reaction parameter.

Acknowledgements

The author thanks the management of Department of Mathematics, Gauhati University for their continuous support to carry out this research work.

Nomenclature

- Br – Brinkman number
- C – concentration
- C_0 – ambient concentration
- C_w – concentration at $\bar{y} = h$
- D – molecular diffusivity
- g – acceleration due to gravity
- Gc – solutal Grashof number
- Gr – thermal Grashof number
- h – half the width of the channel
- K – drag coefficient
- K_0 – thermal conductivity
- P – non-dimensional pressure
- \bar{P} – pressure
- \bar{R} – rate of chemical reaction
- R – non-dimensional chemical reaction parameter
- Sc – Schmidt number
- Sr – Soret number
- T – temperature
- T_0 – ambient temperature
- T_w – temperature at $\bar{y} = h$
- u – non-dimensional solid displacement
- \bar{u} – solid displacement
- v – non-dimensional fluid velocity
- \bar{v} – fluid velocity
- V – average velocity
- (x, y) – non-dimensional Cartesian coordinates
- (\bar{x}, \bar{y}) – Cartesian coordinates
- β – coefficient of heat transfer
- β_C – coefficient of mass transfer
- δ – drag parameter
- λ_J – Jeffrey fluid parameter
- ϕ_f – volume fraction component for the fluid phase
- μ – Lamé constant
- μ_a – apparent viscosity of the fluid in a porous material
- μ_f – intrinsic viscosity of the fluid

- ρ^f – fluid density
 ν_f – kinematic viscosity of the fluid
 Ω – dimensionless ratio of temperature

References

- [1] Bejan A. and Nield D.A. (2013): *Convection in Porous Media*.– 4th edition, Springer.
- [2] Dutta S. and Kalita J.C. (2022): *Heat and mass transfer characteristics of double-diffusive natural convection in a porous annulus: A higher-order compact approach*.– Heat Transfer, vol.51, pp.140-169.
- [3] Kalita B.K. and Choudhury R. (2021): *Flow features of thermophoretic mhd viscous fluid flow past a converging channel with heat source and chemical reaction*.– International Journal of Applied Mechanics and Engineering, vol.26, No.3, pp.72-83.
- [4] Ramzan M., Nisa Z.U., Ahmad M. and Nazar M. (2021): *Flow of Brinkman fluid with heat generation and chemical reaction*.– Complexity, Article ID.5757991, p.11.
- [5] Matta S., Malga B.S., Appidi L. and Kumar P.P. (2021): *Chemical reaction and heat source effects on MHD free convective flow over a linearly accelerated moving vertical porous plate*.– Indian Journal of Science and Technology, vol.14, No.13, pp.1044-1055.
- [6] Vijayaragavan R., Bharathi V. and Prakash J. (2021): *Heat and mass transfer effect of magnetohydrodynamic Casson fluid flow in the presence of inclined plate*.– Indian Journal of Pure and Applied Physics, vol.59, pp.28-39.
- [7] Das U.J. and Das M. (2021): *Unsteady MHD rotating and chemically reacting fluid flow over an oscillating vertical surface in a Darcian porous regime*.– Frontiers in Heat and Mass Transfer, vol.17, p.8, <http://dx.doi.org/10.5098/hmt.17.18>.
- [8] Taid B.K., Ahmed N and Sarma S. (2021): *Heat source and radiation absorption on unsteady MHD fluid flow over an infinite vertical plate embedded in a porous medium in presence of Soret effect*.– Journal of Mathematical Computational Science, vol.11, No.6, pp.7154-7169.
- [9] Das U. (2021): *An unsteady MHD flow of Casson fluid past an exponentially accelerated vertical plate*.– Latin American Applied Research, vol.51, pp.309-314.
- [10] Oomens C. W. J., Van Campen D. H. and Grootenboer, H. J. (1987): *A mixture approach to the mechanics of skin*.– Journal of Biomechanics, vol.20, pp.877-885.
- [11] Biot M. A. (1962): *Mechanics of deformation and acoustic propagation in porous media*.– Journal of Applied Physics, vol.33, pp.1482-1498.
- [12] Barry S. I., Parker K. H. and Aldis G. K. (1991): *Fluid flow over a thin deformable porous layer*.–Journal of Applied Mathematics and Physics, vol.42, pp.633-648.
- [13] Sreenadh S., Rashidi M.M., Kumara Swamy Naidu K. and Parandhama A. (2016): *Free convection flow of a Jeffrey fluid through a vertical deformable porous stratum*.– Journal of Applied Fluid Mechanics, vol.9, pp.2391-2401.
- [14] Murthy M.K. (2020): *Numerical investigation on magnetohydrodynamics flow of Casson fluid over a deformable porous layer with slip conditions*.– Indian Journal of Physics, vol.94, pp.2023-2032.
- [15] Bejan A. (1982): *Entropy generation through heat transfer and fluid flow*.– Wiley, New York.
- [16] Egunjobi A.S. and Makinde O.D. (2013): *Entropy generation analysis in a variable viscosity MHD channel flow with permeable walls and convective heating*.– Mathematical Problems in Engineering, Article ID 630798, p.12, <http://dx.doi.org/10.1155/2013/630798>.
- [17] Das S. and Jana R.N. (2014): *Entropy generation due to MHD flow in a porous channel with Navier slip*.– Ain Shams Engineering Journal, vol.5, pp.575-584.
- [18] Shit G.C., Haldar R. and Mandal S. (2017): *Entropy generation on MHD flow and convective heat transfer in a porous medium of exponentially stretching surface saturated by nanofluids*.–Advanced Powder Technology, vol.28, No.6, pp.1519-1530.
- [19] Sreenadh S., Gopi Krishna G., Srinivas A.N.S. and Sudhakara E. (2018): *Entropy generation analysis for MHD flow through a vertical deformable porous layer*.– Journal of Porous Media, vol.21, pp.523-538.

- [20] Hayat T., Riaz R, Aziz A. and Alsaedi A. (2019): *Analysis of entropy generation for MHD flow of third grade nanofluid over a nonlinear stretching surface embedded in a porous medium.*– Physica Scripta, vol.94, No.12, Article ID 125703, Doi: 10.1088/1402-4896/ab3308.
- [21] Abdelhameed T.K. (2021): *Entropy generation analysis for MHD flow of water past an accelerated plate.*– Scientific Reports, vol.11, Article ID 11964, p.11, <https://doi.org/10.1038/s41598-021-89744-w>.
- [22] Panigrahi L., Panda J. and Sahoo S.S. (2021): *Unsteady heat transfer and entropy generation study on viscoelastic fluid flow coupled with induced magnetic field.*– Iranian Journal of Science and Technology, Transactions A: Science, vol.45, pp.1699-1710.
- [23] Ullah H., Hayat T., Ahmad S. and Alhodaly M.S. (2021): *Entropy generation and heat transfer analysis in power-law fluid flow: Finite difference method.*–International Communications in Heat and Mass Transfer, vol.122, Article ID 105111, p.8, <https://doi.org/10.1016/j.icheatmasstransfer.2021.105111>.

Received: January 28, 2022

Revised: June 3, 2022